39th IAHR WORLD CONGRESS GRANADA, SPAIN 2022 From Snow to Sea 19-24 June 2022

Proceedings of the 39th IAHR World Congress
19–24 June 2022, Granada, Spain
doi://10.3850/IAHR-39WC2521-71192022SS506

Two-Dimensional Depth Averaged Numerical Modelling of Flow Pattern and Sedimentation in Shallow Reservoirs

EL Mehdi CHAGDALI[1], Cédric GOEURY[1], Benjamin DEWALS[2], Sébastien ERPICUM[2], Matthieu SECHER[3],Rem-Sophia Mouradi[1], Kamal EL KADI ABDEREZZAK[1]

[1] National Laboratory for Hydraulics and Environment (LNHE), EDF R&D, Chatou, France.
[2] Research Group of Hydraulics in Environmental and Civil Engineering (HECE), University of Liège, Liège, Belgium.
[3]Hydraulics Engineering Center (CIH), EDF Hydro, La Motte-Servolex, France.

Abstract

Shallow reservoirs are hydraulic structures used for stormwater management or for trapping sediments. Sedimentation in these structures must be minimized or maximized. Sedimentation depends on the flow structures, which in turn depend on the reservoir geometrical shape and its hydro-sedimentary characteristics.In this work, the ability of two-dimensional (2D) depth averaged numerical models using Shallow-Water Equations to simulate flow and sedimentation in shallow reservoirs is examined. Existing laboratory rectangular reservoirs with different locations of inlet and outlet channels and bottom topography (i.e. flat bottom, sediment deposits), are simulated.The model is applied on real shallow basin which operates as a lower basin of a Pumped Storage Hydropower Station.For laboratory cases, a detailed study of the effects of various user-defined numerical model parameters is performed, including the numerical scheme for solving the advection step for velocity and turbulence and the turbulence model. Satisfactorymodel-data agreements are obtained with TELEMAC-2D using the Spalart-Allmaras turbulence model. Simulating the field case, the hydro-sedimentary numerical model TELEMAC-2D coupled with GAIA has been used to explore potential enhancements for the management and maintenance of the basin.A scenario with a deflector placed at the entrance has shownits efficiency in increasing sediment deposits in the northern part of the reservoir where dredging operations can be conducted easily.

Keywords: Flow pattern; Shallow reservoirs; Reservoir sedimentation; Numerical modelling; Sediment transport.

1. INTRODUCTION

Shallow reservoirs are common hydraulic structures widely used for trapping sediment or storing water(Schleiss et al. 2016). They are widely utilized in arid and semi-arid areas as part of Pumped Storage Hydropower Stations(PSHS) (e.g.Morocco, Hatta Pumped Storage Hydroelectric Project in Dubai, Spain, Uzbekistan, Tunisia) (Görtz et al., 2022).Accurate predictions of flow features and location of sediment deposits in reservoirs are crucial for optimal design and management of those structures. Numerical hydro-morphodynamic models are therefore useful tools to meet these needs, as the flow patterns and trap efficiency of a shallow reservoir depend on thereservoir geometrical shape, boundary conditions (i.e. inlet and outlet) and sediment characteristics (Kantoush, 2008; Camnasio et al., 2013).

Flow and sedimentation processes in shallow reservoirs have been studiedusing laboratory experiments insimplified reservoir geometries,numerical modelling, and in less extent through field surveys. Many authors have examined the relation betweenreservoir geometry, boundary conditions and flow patterns, mainly by conducting laboratory experiments with clear water in simplified horizontal (i.e. flat) reservoirgeometries (e.g. rectangular) (see review by Dufresne (2008), Kantoush (2008), Camnasio (2012), among others). Despite the simplified geometry and boundary conditions, complex flow features, 2D or 3D in characters according to the Reynolds number (Durst et al., 1974; Cherdron et al.,1978) have been observed (Kantoush, 2008; Camnasio et al., 2013). Maurelet al. (1996) studied rectangular cavities and observed for low Reynolds numbers three different types of flow, namely a stable regime, a cavity oscillation, and a freejet type oscillation, characterized by a relationship between the Reynolds number and the ratio of reservoir length to inlet diameter. Kantoush (2008) studied experimentally the flow pattern in different shallow rectangular basins under different ranges of Reynolds and Froude numbers, and observed dissymmetric flows in some geometric configurations despite the symmetry of the basin and boundary conditions. Similar observations were found by Camnasio et al. (2013) who confirmed that changing the positions of the inlet and/or outletopen channel leads to very different flow fields.Laboratory experiments in shallow reservoirs with sediment supply have been also conducted, showing the important impact of velocity field distribution, recirculation zones and bottom shear stress on

sediment deposition zones (Stovin and Saul, 1994;Kantoush, 2008). Camnasio et al. (2013) showed that the injection of suspended sediment led to a strongchange in the observed flow field, even with deposit thickness not exceeding 10 % of the water depth.Isenmann (2016)investigated a wide rangeof dimensionless parameters (Froude number, Reynolds number, dimensionless shear stress,dimensional particle diameter)in a cylindric basin with inlet and outlet circular pipes.

Concerning numerical modelling of flow and sediment transport in shallow reservoirs, existingworks mainly focused on evaluating theability of numerical codes to reproduceexperimental laboratorymeasurements.Kantoush(2008) and Camnasioet al. (2013) showed that 2D modeling based on the Saint-Venant equations correctly simulatedthe flow pattern in a shallow rectangular basin. Using the same numerical model, satisfactory model-data agreement was found for meandering jet by Peltieret al. (2014).Codes solving Navier-Stokes equations havealso been used to validate laboratory configurations.For example, Dufresne (2008) usedanEuler-Lagrangian approach for simulating sediment transport in a rectangular reservoir with a circular pipe at the inlet and a frontal weir at the outlet. Esmaeili et al. (2015) studied the 3D velocity field in rectangular shallow reservoirs with different geometries for flat bottom and bottom with sediment deposits. Overall, the experimental flow fields were reproduced with a good accuracy. An open source code was used by Isenmann (2016) to reproduce laboratory experiments of flow and sediment transport in shallow reservoirs.A good model-data agreement is found for estimating thetrapping efficiency.Some studies focused onthe improvement of reservoir performance using numerical models. Persson(2000) evaluated the hydraulic efficiency of thirteen shallow basins with 2Dnumerical modeling and found that the presence of an obstacle in front of the basin entrance could increase their trapping efficiency. Using 2D numerical model, Ferrara et al. (2018) evaluated the effect of varying the inletand outlet position on flow field for rectangular shallow basins. Using 3D numerical model, Zahabi et al. (2018) evaluated the effects of geometry, position of boundary conditions and flow characteristics on trapping efficiency.

Few real reservoir studieshave been treated in the literature.Yan (2013) used a three-dimensional(3D) modelto simulatedflow in a largesettling reservoir. Claude et al.(2019)performed a 3Dhydro-sedimentary numerical study on a real shallow reservoir using TELEMAC-3D. The codecapturedaccuratelytheglobal behavior of the hydrodynamic and sediment transport. As presented previously for laboratory cases, some studies have been conducted to enhance the performance of real reservoir. Using 2D hydrodynamic and water quality transport models.Koskiaho (2003) proposed modifications for two retention reservoirs in order to avoid the formation of dead zones. Using 3D codes, Stamou (2008) studied the increase in hydraulic efficiency through modifying the geometry of nine basins.

This paper is mainly oriented to hydro-sedimentary numerical modelling using theopen sourcesuite of codes TELEMAC-MASCARET. The aim of this workis to show the ability of 2D depth averaged numerical model using Shallow-Water Equations TELEMAC-2D to simulate flow and sedimentation in shallow reservoirs and secondly, to explore potential enhancements for the management and maintenance of a real basin with a guide wall design. The remainder of this paper is structured as follows: in Section 2, numerical simulationsof Camnasio et al.'s (2013) laboratory experimentsare performed.In Section 3,the Cheylas reservoir is studied, followed by concluding remarks.

2. NUMERICAL MODELLING OF LABORATORY EXPERIMENTS

Laboratory experiments conducted by Camnasio et al. (2013)are simulated. The experimentalsetup consisted of a rectangular PVC basin, L = 4.5 m long and B = 4 m wide, and two rectangular free surface channels, l = 1 m long and b = 0.25 m wide each (Figure. 1). In the present work, four configurations are simulated (Figure 1), referred to C-C(symmetric case), L-L, L-R and C-R (asymmetric cases), respectively.

A constant clear water discharge of Q = 7 L/s is imposed at the inlet channel, while a flap gate located at the outlet channel end regulated the flow depth in the reservoir at h = 0.2 m. The Froude and Reynolds numbers in the inlet channel are F_{in}= 0.1 and R_{in}= 112 000, respectively.The sameexperiments were repeated while feeding the inlet channel continuously with crushed walnut shells (density $Á_s$ = 1500 kg/m^3, median diameter d_{50} = 89µm) at a mean inflowing concentration of C_{in}= 2 g/l. The horizontal velocity field was measured using Ultrasonic Velocity Profiler(UVP) () transducers placed at 8 cm (= 0.4h) from the bottom.The thickness of sediment deposits inthe reservoir was measured by a laser technique after 2 h and 4 h of sediment feeding

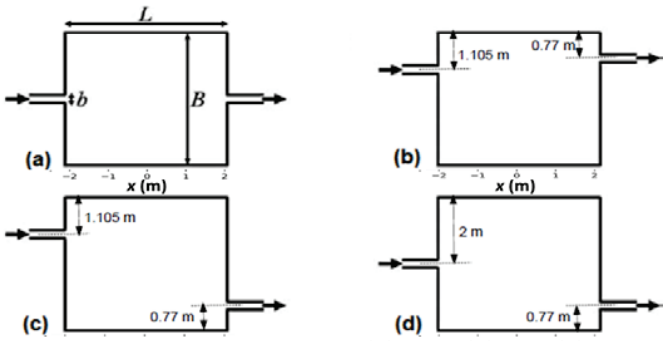

Figure 1. Plane view of laboratory configurations: (a) C-C, (b) L-L, (c) L-R, and (d) C-R

The simulations are performed with the finite element version of the depth-averaged TELEMAC-2D hydrodynamic model (V8P2), which solves the Saint-Venant equations (El kadi Abderrezzak et al., 2016). For all the configurations, a Strickler formula with a coefficient equal to 80 $m^{1/3}s^{-1}$(corresponding to PVC) is used. The effect of sidewall friction was tested and no influence on the numerical results was noted. A CFL number lower than 0.8 isused, and a grid size of 0.025 m is retained according toa mesh convergence study. The numerical model is first used to simulate the “clear water” cases (i.e. reservoir flat bottom). Then, the model is used to simulate the flow field in the reservoir with the measured bathymetry after 4 h of sediment supply.For the sake of brevity, only selected results are shown.

For clear water tests, several numerical schemes for solving the advection step for velocity and turbulence are compared: method of characteristics, N distributive scheme, Positive Streamwise Invariant (PSI), PSI scheme with Locally semi-Implicit Predictor-corrector Scheme (LIPS), and Element by element Residual distributive Iterative Advection scheme (ERIA). The effect of numerical scheme is illustratedin Figure 2 for C-C configuration. The effect of numerical schemes is weak, and this finding remains valid for all configurations and turbulence models.The LIPS is chosen for the rest of the study, as the scheme is less diffusive.

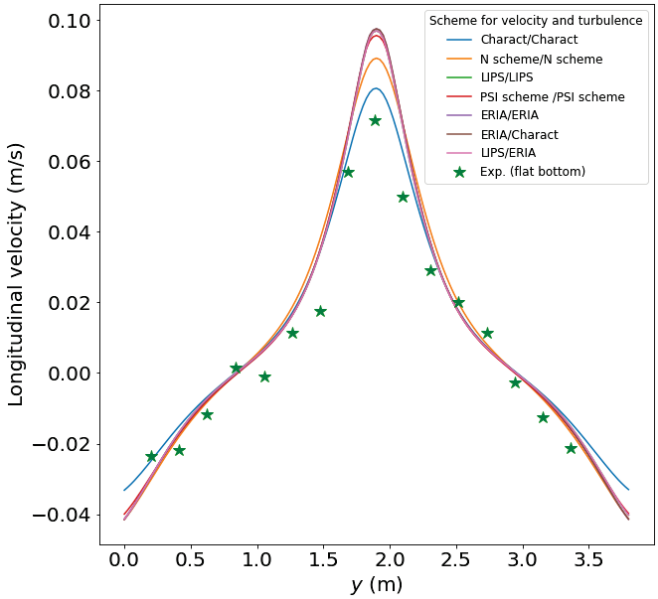

Figure 2. C-C configuration: Measured and computed cross-sectional profiles of longitudinal velocity at *x*= 1.73 m with different numerical schemes for advection of velocity and turbulence. Flat bottom, k–μ turbulence model and mesh size of 0.025 m

Figure 3 shows a comparison betweenexperimental and computed velocity fields for C-C, C-R, L-L and L-R configurations (clear water, i.e. flat bottom) using Spalart-Allmaras(Bourgoin et al., 2021), k–μ, Elder turbulencemodels and constant viscosity (10^{-3} m^2 s^{-1}). The Spalart-Allmaras turbulence model provides satisfactory results of flow pattern for the four configurations. The k–μ, Elder and constant viscosity(10^{-3} m^2 s^{-1}) turbulence modelsyield satisfactory results for C-C, L-L and C-R configurations, but do not allow replicating the reattachment point on the left sidefor the L-Rconfiguration. The simulation of this case was very sensitive to the initial conditions. A simulation using the k–μ turbulence model employing a steady flow pattern with lateral reattachment as initial conditions allowreproducing well the experimental flow pattern. Similar results were obtained by Camnasio et al. (2013).

Figure 4 shows the longitudinal velocity profiles for different turbulence models.The k–μ and Elderturbulence models reproducethe shape of measurements accurately but overestimate the velocity peak.

The Spalart-Allmaras and constant viscosity (10^{-3} m² s^{-1}) turbulence models reproduce less well the shape of measurement andunderestimate thevelocity peak.Finally, it can be concluded that Spalart-Allmaras (SA)model stands out from other turbulence models because it could correctly predict the velocity fields of the four cases without changing the initial conditions.

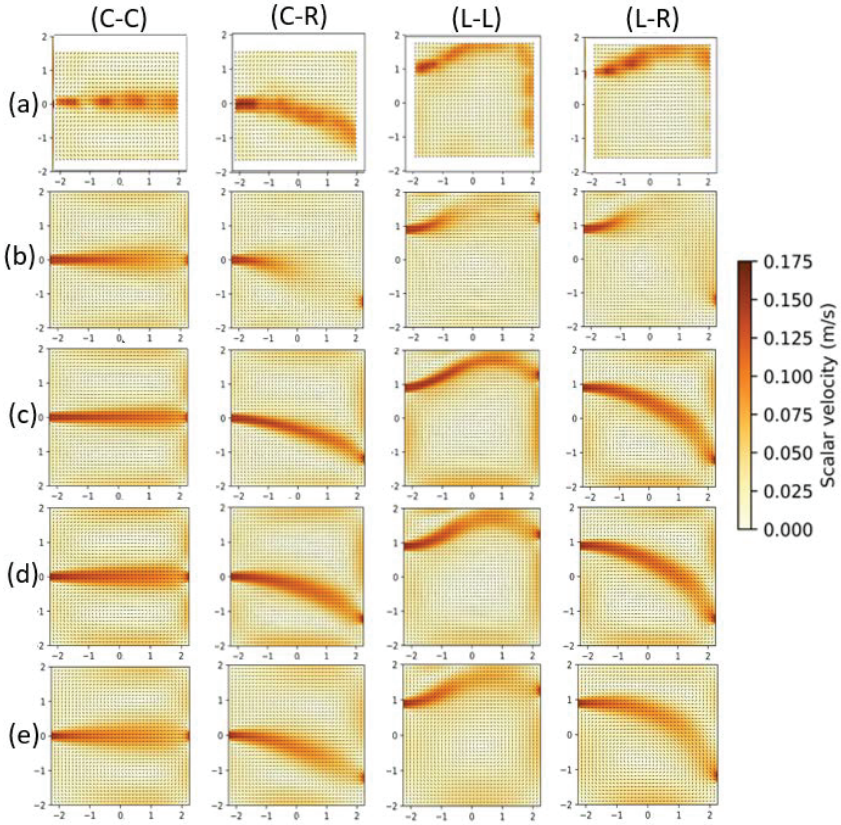

Figure 3. Experimental (a) and computed velocity fields for C-C, C-R, L-L and L-R configurations using (b) Spalart-Allmaras model, (c) k–μ model, (d) Elder model,and (e) constant viscosity (10^{-3} m² s^{-1}) model. Flat bottom, LIPS and mesh size of 0.025 m

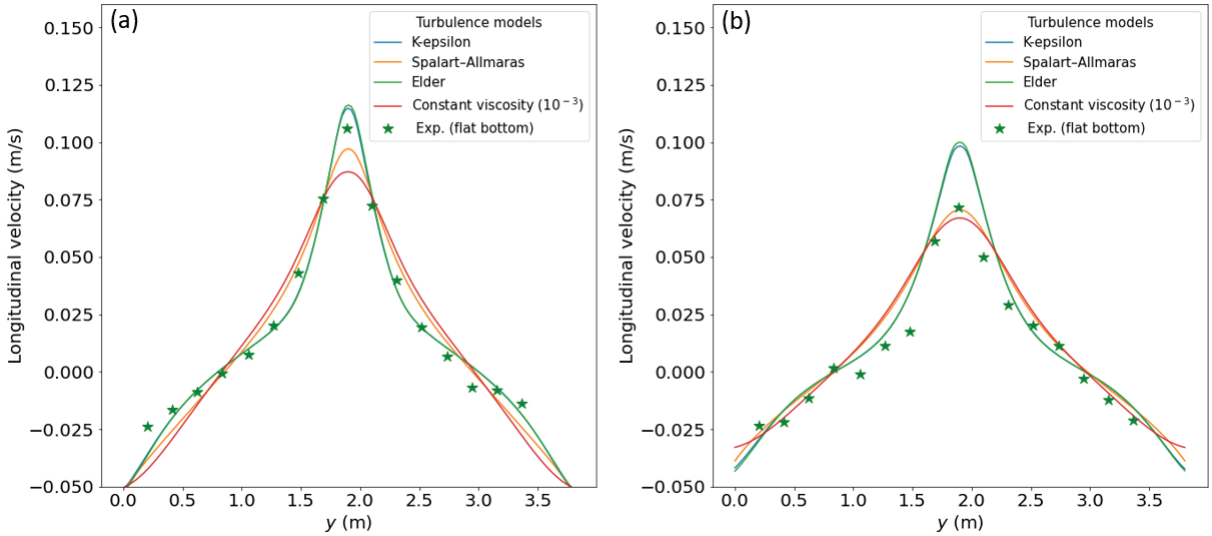

Figure 4. C-C configuration: measured and computed cross-sectional profiles of longitudinal velocity at (a) x = 0.71 m, and (b) x= 1.73 m withdifferent turbulence models. Flat bottom, LIPS and mesh size of 0.025m

The influence of bottom topography on flow pattern is analyzed while adding a bathymetry equivalent to the sediment deposits thickness after 4h for C-C configuration (Figure 5). Figure 6plotsmeasurements and computed longitudinal velocity profiles usingk–μ, Spalart-Allmaras (SA),constant viscosity (10^{-3} m² s^{-1}) and Elder turbulence models.Similar conclusions to the configuration presented previously with a flat bottom are

found,except with the k–μturbulence model which presents an unsteady regime for the case with sediment deposit. This regime can be observed on Figure 6by a slight deviation of the position of the velocity peak.

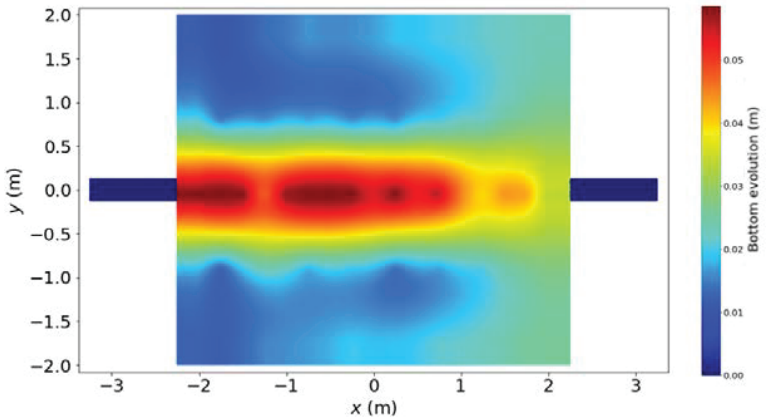

Figure 5. Bottom elevation after 4 hof sediment supply for C-C configuration

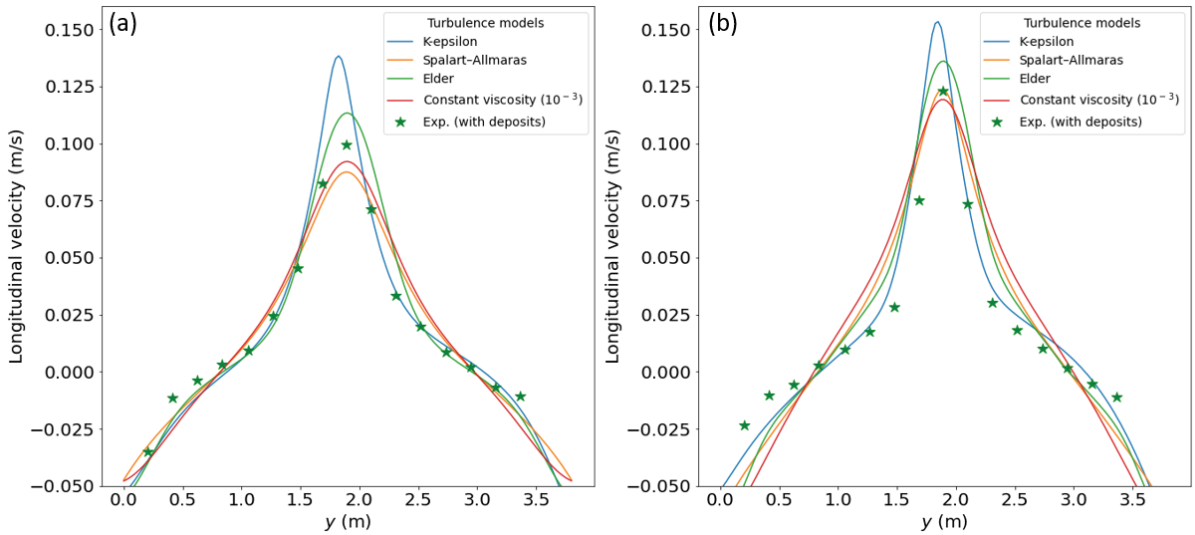

Figure 6. C-C configuration: measured and computed cross-sectional profiles of the longitudinal velocity at (a) x= 0.71 m, (b)x= 1.73 m. Reservoir with deposits, LIPS and mesh size of 0.025 m

3. NUMERICAL MODELLING OF FIELD CASE

The capacity of Cheylas real basin to be used as a sediment transit basin has been studiedby Claude et al. (2019) using in-situ measurements and numerical models. The ability of TELEMAC-2D-SISYPHEand TELEMAC-3D-Sedi3D (SISYPHE and Sedi-3D are,respectively, the 2D and 3D old sediment transport modules in the TELEMAC-MASCARETchain) to reproduce the flow structure and sediment transfer in this basin was studied. In this work, this setup has been adapted to TELEMAC-2D and GAIA (the new 2D sediment transport module in TELEMAC-MASCARETsuite).

An exploratory study of potential enhancement of the management and maintenance of the Cheylas basinby adding deflectors is conducted.The objective of the addition of deflectors is to favor deposits of sediment in the northern part of the basin in order to facilitate the dredging operations.The calculation is performedwhile coupling hydrodynamic moduleTELEMAC-2Dand sediment transport module GAIA. The mesh is unstructured with a total number of nodes equal to 155000 (Figure 7). For TELEMAC-2D module, k–μ turbulence model and LIPS scheme are used, aCFL number is chosen lower than 0.8.A flow discharge of 98 m^3/s is imposed at the inlet boundary, which isin the form of pressurized jet, anda water level of 242.33 m is prescribed at the outlet boundary.Accordingthe calibration set-up byClaude et al. (2019), a Strickler formula is used with a coefficient set at55 $m^{1/3}s^{-1}$.

For GAIA module, suspended sediment is governed by the vertically averaged advection-diffusion equation. The laws used to calculate the erosion E and deposition D fluxes are as:

- Partheniades'slaw for erosion flux: if the bottom shear stress $\tau$is larger than the critical shear stress for initiation of motion τ_{ce} ($\tau > \tau_{ce}$), then $E=M((\tau/\tau_{ce}-1)$; otherwise E = 0, with MPartheniades's coefficient.

- Krone's law for deposition flux: if the bottom friction velocity u_* is lower than the critical shear velocity for deposition u_{*d} ($u^*<u^*_d$), then, $D=W_sC[1-(u_*/ u_{*d})]^2$, with W_s cohesive sediment settling velocity and C average volumetric sediment concentration.

According to Claude et al. (2019) the diffusion of suspended sediment is equal to zero, the volumetric concentration of the bed is fixed at 1000 kgm^{-3}, the critical erosion stress is τ_{ce}= 1 Pa, and the Partheniades constant M = 0.01 kg m^{-2} s^{-1}.The settling velocity is computed according to the concentration (Claude et al. 2019).Bed load transport is not considered, sediment is assumed cohesive with D_{50}= 10^{-2} mmand sediment density equal to 1600 kg/m^3. A concentration of 0.25 g/l is imposed at the inlet boundary, which is an operating value. The calculation time is equal to 10 hours.In the first scenario, a deflector is added at the entrance, while in the second option the deflector is placed perpendicular to the flow direction (Figure 8). Deflectors are implemented in the numerical modelby raising locally the reservoir bathymetry.

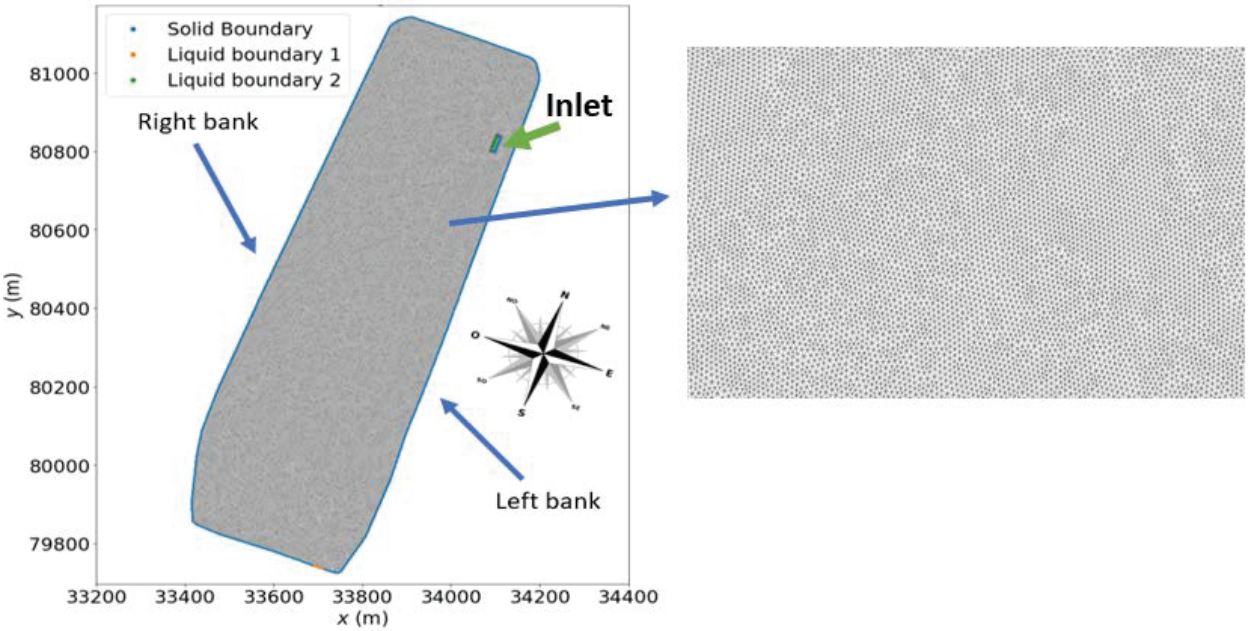

Figure 7.Unstructured 2D mesh and boundary conditions positions for Cheylas real basin

Figure 8 shows locations of Deflectors 1 (i.e. structure at the entrance) and 2 (i.e. structure perpendicular to the right bank) and the initial flow depth conditions. Thewater heightat the entrance is higher (+17.5 m) than the average water-depth in the basin, which could be explained by the erosion effects due to high flowrate from the inlet jet.

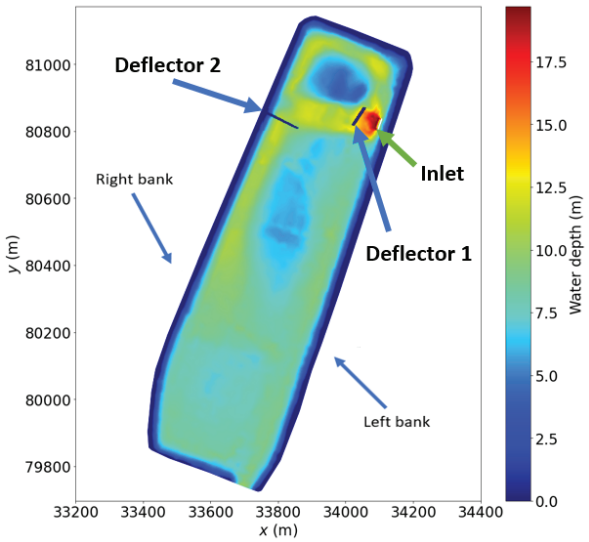

Figure 8. Initial flow depth and position of deflectors: Deflector 1(at the entrance) and Deflector 2 (perpendicular to right bank)

Without any deflector (Figure 9 (a)), the simulated flow pattern results show a recirculation in the north, generated by the outflow from the inlet jet in a direction perpendicular to the basin length axis. The main inlet jet splits in two at the right bank of the basin. The major part of the jet leaves toward the south and sticks to the bank before joining the outlet of the basin. This generates a large recirculation on the major part of the Cheylasreservoir on the left bank.As displayed in Figure 9 (b) and (c), deflectors allow a change in the position of spiling flow point which implies a change in main jet direction. The recirculation in the north is impacted by the deflectors.Its size, shape and magnitude change specifically for case with deflector placed at the reservoir inlet. A meandering jet is found for the three studiedconfigurations.

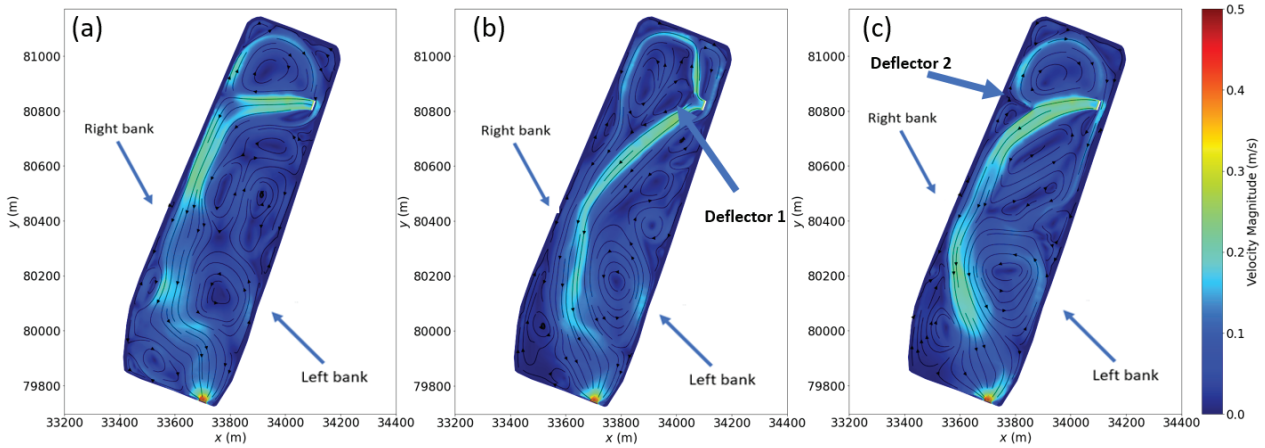

Figure 9. Simulated velocity for (a) real case, (b) reservoir with Deflector 1 at entrance, and (c) reservoir with Deflector 2 at bifurcation point, at t = 10 h

Figure 10 showsthe positive bottom evolution due to sediment deposits after 10 hours of simulation; the negative evolution of the bathymetry due to erosion is not presented. The deposit of interest is inthe northern part of the yellow barpresented on Figure 10. The results show that areas of sediment accumulation are closely related to the flow pattern, as sediments are deposited in the jet principal direction. The placement of Deflector 1 at the level of the entrance of the jet makes possible to meet the principal objective which is to support the deposit in the northern part of the reservoir. The flow splits at the deflector level and thus implies that the flow goes directly to the northern part of the basin. On the other hand, Deflector 2placed close to the right bank and perpendicular to the flow direction, which is placed in a perspective to block the split point in the initial configuration, does not achieve the desired objective.

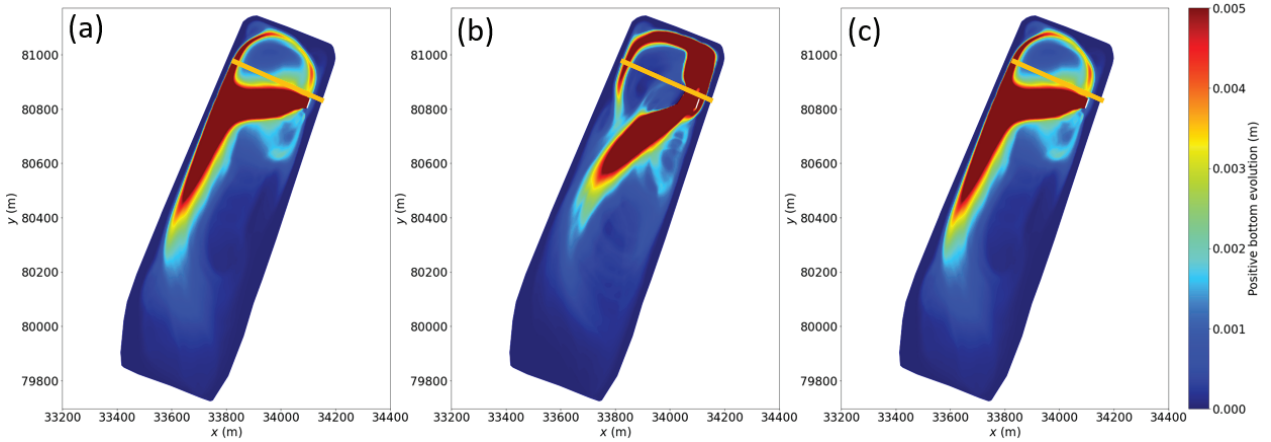

Figure 10. Positive bottom evolutionfor (a) real case, (b) reservoir with Deflector 1 at the entrance, and (c) reservoir with Deflector 2 at bifurcation point,at t = 10 h

To quantitively evaluate the impact of adding a deflector on sediment deposits, the positive volume of deposition in the northern part of the reservoir after 10 h of simulation is presented in Figure 11. The scenario with Deflector1 in front of the inlet boundary condition gives better results, with higher sediment deposits and clearly stands out from the other scenario. The addition of a deflector at the inlet boundary condition allows increasing the sediment deposits in the northern part of reservoir by more than three times. A more judicious choice of the position and size of the deflector with geometrical optimization methods would certainly allow furtherimproving of theseresults.

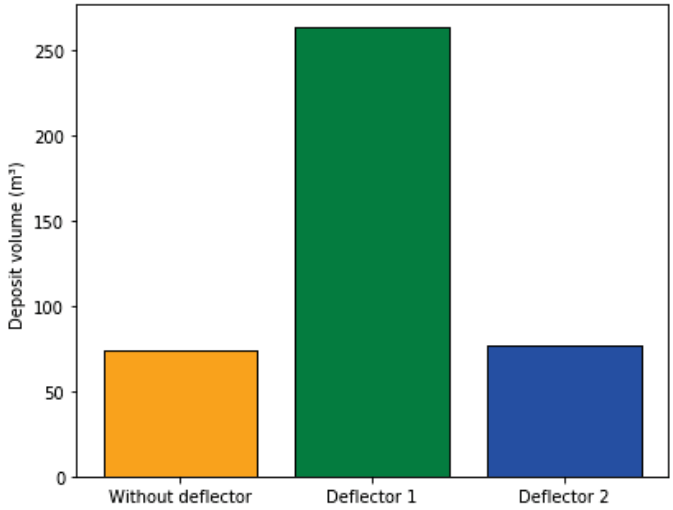

Figure 11. Positive volume (m^3)at the north of the reservoir according to three scenarios

4. CONCLUSIONS

A numerical modelling of shallow rectangular reservoir is performed using TELEMAC-2D. For all laboratory configurations performed with clear water (flat bottom), satisfactory model-data agreements are obtained with TELEMAC-2D using the Spalart-Allmaras turbulence model. The k–μ, Elderand constant viscosity (10^{-3} m^2 s^{-1}) turbulence models yield satisfactory model-data agreementand a goodreproductionof velocity magnitudes for C-C, L-L and C-R configurations, but do not allow replicating the point of attachment for configuration L-R. TELEMAC-2D allow a good representation of bathymetric effect on the shallow reservoir.

The hydro-sedimentary numerical model TELEMAC-2D coupled with GAIAshows its ability to reproduce the global flow structure and sediment transport processes at the reservoir scale. Adding deflectors is conducted to explore potential enhancements for the management and the maintenance of the basin. Three scenarios are compared. A solution with a deflector at the entrance of the reservoir increases the accumulation of sediment in the northern part of the reservoirwhere dredging operation can be conducted easily. Future work will include application of the hydro-morphodynamical model TELEMAC-2D coupled to GAIAto simulate thelaboratory experiments with sediment supply and optimizationof the position and shape of the deflector.

5. ACKNOWLEDGEMENTS

This work is partially funded by Association Nationale de Recherche et de la Technologie (ANRT) [CIFRE #2019/1262].

6. REFERENCES

Bourgoin, A., El kadi Abderrezzak, K., Benhamadouche, S., and Ata, R., (2021). An adoption of the Spalart–Allmaras turbulence model for two- and three-dimensional free surface environmental flows. *Journal of Hydraulic Research*, 59(2), 314-328.

Camnasio, E., Erpicum, S., Orsi, E., Pirotton, M., Schleiss, A.J., and Dewals, B. (2013). Coupling between flow and sediment deposition in rectangular shallow reservoirs. *Journal of Hydraulic Research*, 51(5), 535-47.

Choufi, L., Kettab, A., andSchleiss, A.J. (2014). Effet de la rugosité du fond d'un réservoir rectangulaire à faible profondeur sur le champ d'écoulement (Effect of bottomroughness of a shallowrectangularreservoir on the flow field).*La Houille Blanche*, 83-92.

Claude, N., Secher, M., Deng, J., Valette, E., and Duclercq, M. (2019). 2D and 3D numerical modelling of the flow and sediment transport in shallow reservoirs: application to a real case.*XXVIthTelemac& Mascaret User Club*.

Dufresne, M. (2008). La modélisation 3D du transport solide dans les bassins enassainissement : du pilote expérimental à l'ouvrage réel.(3D modeling of solid transport in wastewater basins: from experimental pilot to real reservoir).*Doctoral dissertation*,Université Louis Pasteur, Strasbourg, France.

Dewals, B., Kantoush, S., Erpicum, S., Pirotton, M., andSchleiss, A.J. (2008). Experimental and numerical analysis of flow instabilities in rectangular shallow basins. *Environmental Fluid Mechanics*, 8, 31-54.

El kadi Abderrezzak, K., Die Moran, A., Tassi, P., Ata, R., and Herouvet, J.M. (2016). Modelling river bank erosion using a 2D depth-averaged numerical model of flow and non-cohesive, non-uniform sediment transport. *Advances in Water Research*, 93(A), 75-88.

Esmaeili, T., Sumi, T., Kantoush, S., Haun, S., and Rüther, N. Three-dimensional numerical modelling of flowfield in shallow reservoirs. (2015). *ICE-Water Management,* 169, 229-244.

Ferrara, V., Erpicum, S., Archambeau, P., Pirotton, M., and Dewals, B. (2018). Flow field in shallow reservoir with varying inlet and outlet position. *Journal of Hydraulic Research*. 56, 689-696.

Frey, P., Champagne, J.Y., Morel, R., and Gay, B. (1993). Hydrodynamics fields and solid particles transport in a settling tank. *Journal of Hydraulic Research,* 31(6), 736-776.

Görtz, J., Aouad, M., Wieprecht,S., and Terheiden, K. (2022). Assessment of pumped hydropower energy storage potential along rivers and shorelines. Renewable and Sustainable Energy Reviews, 112027.

Isenmann, G. (2016). Approche Euler–Lagrange Pour la Modélisation du Transport solide dans les ouvrages de décantation. (Euler-Lagrange Approach for Modeling Solid Transport in Settling basins). *Doctoral dissertation,* Université de Strasbourg, France.

Kantoush, S.A. (2008). Experimental study on the influence of the geometry of shallow reservoirs on flow patterns and sedimentation by suspended sediments. *Doctoral dissertation*,Laboratoire de Constructions Hydrauliques, EPFL, Switzerland.

Koskiaho, J. (2003). Flow velocity retardation and sediment retention in two constructed wetland-ponds.*Ecological Engineering*, 19, 325-337.

Maurel, A., Ern, P., Zielinska, B., and Wesfreid, J.E. (1996). Experimental study of self-sustained oscillations in a confined jet. *Physical Review*, 54(4), 3643-3651.

Peltier, Y., Erpicum, S., Archambeau, P., Pirotton, M., and Dewals, B. (2014). Experimental investigation of meandering jets in shallow reservoirs. *Environmental Fluid Mechanics*,14(3), 699-710.

Persson, J. (2000). The hydraulic performance of ponds of various layouts. *Urban Water*, 2, 243-250.

Schleiss, A.J., Franca, M.J., Juez, C., and De Cesare, G. (2016). Reservoir Sedimentation. *Journal of Hydraulic Research,* 54, 595-614.

Stamou, A. (2008). Improving the hydraulic efficiency of water process tanks using CFD models. *Chemical Engineering and Processing: Process Intensification*, 47(8), 1179-1189.

Stovin, V.R., and Saul, A.J. (1994). Sedimentation in Storage Tank Structures. *Water Science andTechnology*,29, 363-37.

Yan, H. (2013). Experiments and 3D modelling of hydrodynamics, sediment transport,settling andresuspension under unsteady conditions in an urban stormwaterdetention basin. *Doctoral dissertation*,Institut National des Sciences Appliquées (INSA) de Lyon, France.

Zahabi, H., Torabi, M., Alamatian, E., Bahiraei, M., andGoodarzi, M.(2018). Effects of geometry and hydraulic characteristics of shallow reservoirs on sediment entrapment. *Water*, 10(12), 1725.

